

Effect of Passive Reflectors for Enhancing Coverage of 28 GHz mmWave Systems in an Outdoor Setting

Wahab Ali Gulzar Khawaja¹, Ozgur Ozdemir¹, Fatih Erden¹, Ismail Guvenc¹, Martins Ezuma¹ and Yuichi Kakishima²

¹Department of Electrical and Computer Engineering, North Carolina State University, Raleigh, NC

²DOCOMO Innovations, Inc., Palo Alto, CA

Email: {wkhawaj, oozdemi, ferden, iguvenc, mcezuma}@ncsu.edu, kakishima@docomoinnovations.com

Abstract—The availability of large unused spectrum at millimeter wave (mmWave) frequency bands has steered the future 5G research towards these bands. However, mmWave signals are attenuated severely in the non-line-of-sight (NLOS) scenarios, thereby leaving the strong link quality by a large margin to line-of-sight (LOS) links. In this paper, a passive metallic reflector is used to enhance the coverage for mmWave signals in an outdoor, NLOS propagation scenarios. The received power from different azimuth and elevation angles are measured at 28 GHz in a parking lot setting. Our results show that using a 33 inch by 33 inch metallic reflector, the received power can be enhanced by 19 dB compared to no reflector case.

Index Terms—Coverage, mmWave, non-line-of-sight (NLOS), outdoor, reflector.

I. INTRODUCTION

There has been a surge in the use of smart communication devices in recent years. For example, in the U.S. the percentage of the population owning a smart phone has increased from 35% in 2011 to 77% in 2018 [1]. These smart devices can support high data rate applications that are becoming an essential part of the everyday life. However, due to increasing congestion at the sub-6 GHz spectrum, it is difficult to support high data rate applications in the future. This motivated the cellular industry to explore millimeter wave (mmWave) frequency bands for mobile communications. Major hurdles for mmWave based system implementation include high free space attenuation, limited signal penetration through building structures, and small diffraction from large structural edges. This makes the radio signal planning for non-line-of-sight (NLOS) paths very difficult.

There are numerous solutions proposed in the literature in order to overcome the hurdle of high attenuation at the mmWave frequency bands, especially, for NLOS paths. These solutions include beam-forming and beam-steering techniques using multiple antennas, high transmit power and high sensitivity receivers, and use of multiple active repeaters. However, all of these solutions have limitations.

This work has been supported in part by NASA under the Federal Award ID number NNX17AJ94A and by DOCOMO Innovations, Inc. We also thank Fujio Watanabe and Masato Takada from DOCOMO Innovations, Inc. for their valuable feedback in this study.

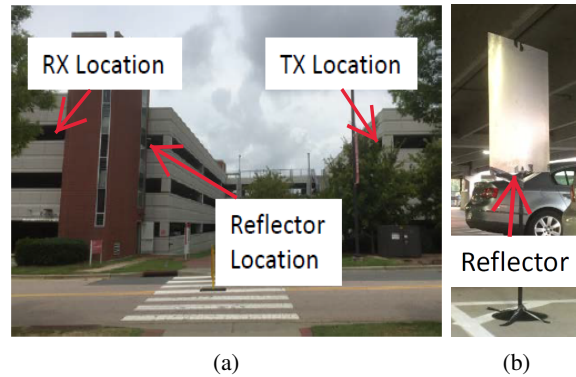


Fig. 1: Measurement setup (a) Overview of the measurement setup (b) 33 in \times 33 in metallic reflector.

Complex, expensive and high power consumption devices are required for beam-forming and beam-steering and it can still suffer in the NLOS propagation. Similarly, due to limitations on the transmit power emission by regulatory bodies, the transmit power can not be increased beyond a given value. Furthermore, using high sensitivity receivers and multiple active access points may not be economically and practically convenient.

A feasible and more economical solution not extensively studied in the literature for mmWave signal enhancement in the NLOS scenarios is by using simple metallic passive reflectors in the propagation path. The properties of electromagnetic wave propagation are similar to the light [2]. Therefore, similar to light reflection principle, metallic reflectors can be used to reflect the electromagnetic waves. These electromagnetic wave reflections from metallic objects are better at higher frequencies due to smaller skin depth [3], owing to lower material penetration. These metallic reflectors in the propagation link behave somewhat similar to a communication repeater. They also have the advantage of using no electricity and small initial investment, compared e.g. to wireless repeaters. Furthermore, they require negligible maintenance, have long life spans, and can also be part of common real life objects such as advertisement boards, lamp posts, and street signs.

There are limited studies available in the literature on using passive reflectors for downlink communications [4],

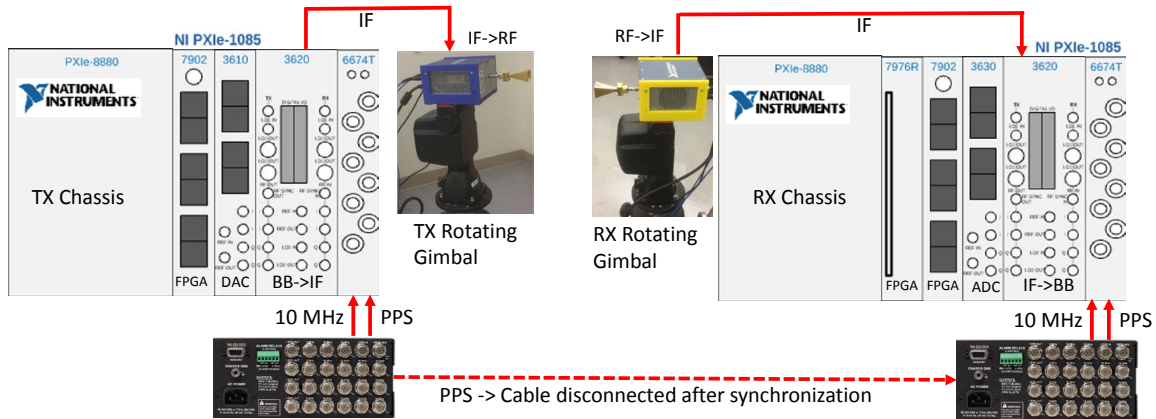


Fig. 2: 28 GHz channel sounder TX and RX hardware setup.

[5]. Passive reflectors were mostly used in the past for point-to-point long distance links [6]–[8] and is main focus of radar research studies [9]–[11]. In our recent work [12], [13], metallic passive reflectors of different shapes/sizes were used to enhance the coverage of NLOS scenarios in mmWave systems. A median gain of 20 dB was observed with flat metallic reflector as compared to no reflector, whereas a cylindrical metallic reflector was found to provide more uniform coverage over the receiver grid. In [14], numerical analysis was carried out to observe the effect of a parabolic reflector placed on top of a building. The base station was placed on another building opposite to the reflector. The parabolic reflector was found to overcome the shadowed regions between the buildings.

In this work we study the effect of reflectors on enhancing the coverage of mmWave systems in an outdoor setting as shown in Fig. 1. A rotating gimbal is used to measure the received power from different directions in a parking lot. The measurement results show that around 19 dB power gain is achieved with the reflector, when compared to the communication link with no reflector.

II. HARDWARE SETUP

The measurements were performed using NI mmWave PXI platforms at 28 GHz [15]. The hardware setup is shown in Fig. 2. The 10 MHz and pulse per second (PPS) signals generated by FS725 Rubidium (Rb) clocks [16] are connected to PXIe 6674T modules at the transmitter and the receiver. The PPS output from one of the clocks is connected to the PPS input of the other clock so that the two clocks are synchronized before the carrying out the measurements. Once the clocks are synchronized, this connection can be removed so that the transmitter and the receiver can be separated from each other without any cable connecting them.

Zadoff-Chu (ZC) sequence of length 2048 is periodically transmitted to sound the channel. The sounder has two modes of operation: 1 GHz and 2 GHz. In 2 GHz mode of operation which is used during these measurements, ZC sequence is over-sampled by 2 and filtered by root raised cosine (RRC) filter and the generated samples are uploaded

into FPGA denoted by PXIe-7902. These samples are sent to PXIe-3610 digital to analog converter (DAC) with a sampling rate of $f_s = 3.072$ GS/s. The PXIe-3620 module up-converts the base-band signal to IF and 28 GHz mmWave radio head up-converts the IF signal to RF.

Directional horn antennas [17] are connected to the mmWave radio heads at the transmitter and receiver sides with 17 dBi gains and 26° and 24° beam-widths in the elevation and azimuth planes, respectively. The transmitter and receiver mmWave radio heads are placed on FLIR PTU-D48E gimbals [18] in order to measure the angular profile of the channel.

At the receiver side, 28 GHz mmWave radio head down-converts the RF signal to IF. The IF signal is down-converted to base-band at the PXIe-3620 module. The PXIe-3630 analog to digital converter module samples the base-band analog signal with the sampling rate of $f_s = 3.072$ GS/s. The correlation and averaging operations are performed in PXIe-7976R FPGA operation and the complex channel impulse response (CIR) samples are sent to the PXIe-8880 host PC for further processing and saving to local disk.

When the oversampling by two is performed, the channel sounder provides $2/f_s = 0.65$ ns delay resolution in the delay domain. The analog to digital converter has around 60 dB dynamic range and path loss up to 185 dB can be measured.

A. Calibration for Non-Ideal Hardware Response

One of the challenges when performing wide-band channel sounding is that the measurement hardware itself may introduce channel distortions which should be calibrated. One expects a flat response when a calibration cable is connected between the transmitter and the receiver as shown in Fig. 3(a). However, due to the non-idealities of the hardware, spurs can be observed at the power delay profile (PDP) as seen in the example in Fig. 3(b). By connecting the transmitter and the receiver with a calibration cable, it is possible to measure and calibrate the non-flat frequency response of the hardware. During this measurement a 40 dB attenuator is used to protect

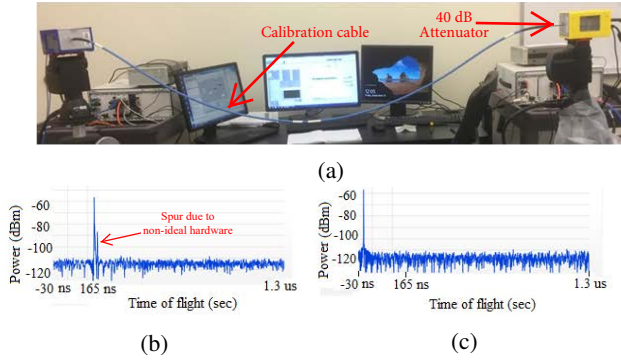


Fig. 3: Calibration for hardware non-ideal hardware response, (a) Calibration cable connected between transmitter and receiver mmWave radio heads (b) PDP obtained due to non-ideal hardware (c) PDP after calibration of the non-ideal hardware response

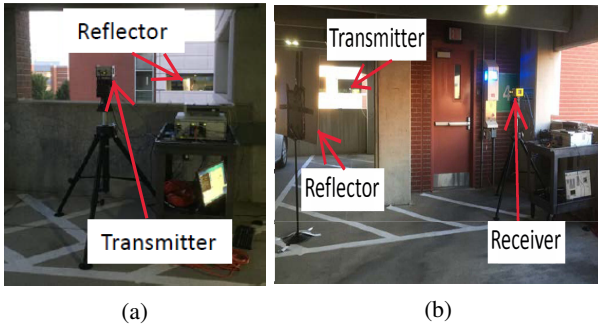


Fig. 4: Measurement setup: (a) The transmitter shown on the gimbal; during the measurements, the transmitter was not rotated. (b) Receiver location; the reflector is positioned at 45° angle to maximize the received power.

the receiver when a signal with high power is transmitted. Fig. 3(c) shows the response after calibration is performed where no spur is observed.

III. MEASUREMENT SETUP

The measurements were performed inside two parking buildings next to each other at North Carolina State University (NCSU) campus as shown in Fig. 4. The receiver is located behind brick walls surrounding the stairs so that there is no direct line of sight (LOS) path between the transmitter and the receiver. A passive metallic reflector of size 33 inch by 33 inch is used 4.5 m away from the receiver as shown in Fig. 5. The receiver antenna is mounted on a rotatable gimbal in order to collect energy from different directions.

For comparison we consider two scenarios: one without reflector and one with reflector as shown in Fig. 6. The transmitter is not rotated and its position is fixed at 90° elevation angle *facing the location of the reflector*. We adjust the heights of the transmitter and receiver equal to each other so that it is expected that the received power will be maximum when the receiver is at 90° elevation angle as shown in Fig. 7. The gimbal at the receiver side

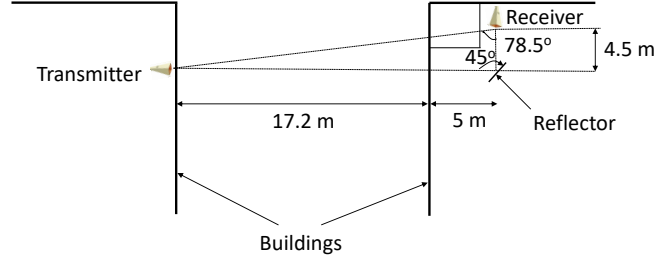


Fig. 5: Top view of the layout of the measurement scenario with the heights of the transmitter and receiver at 1.5 m and the reflector center is aligned to the center of the transmitter/receiver antenna.

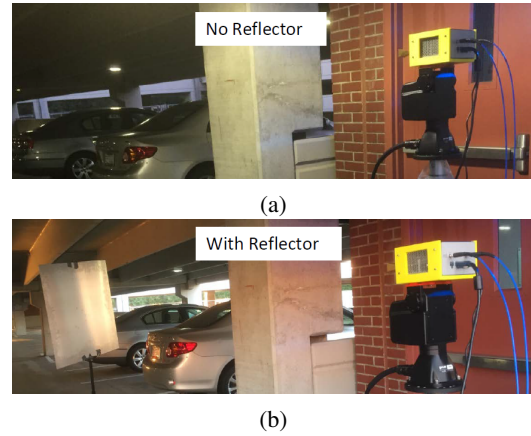


Fig. 6: Scenarios with: (a) no reflector, (b) with reflector.

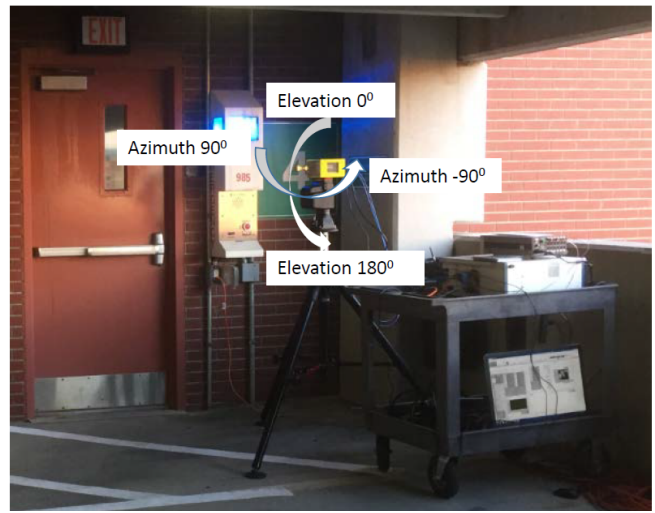


Fig. 7: The orientation of elevation and azimuth angles

scans the azimuth plane from -165° to 165° with 10° increments and the elevation plane from 1° to 119° with 10.7° increments.

IV. MEASUREMENT RESULTS

The transmit power is set to 20 dBm during measurements. For each antenna position the total received power

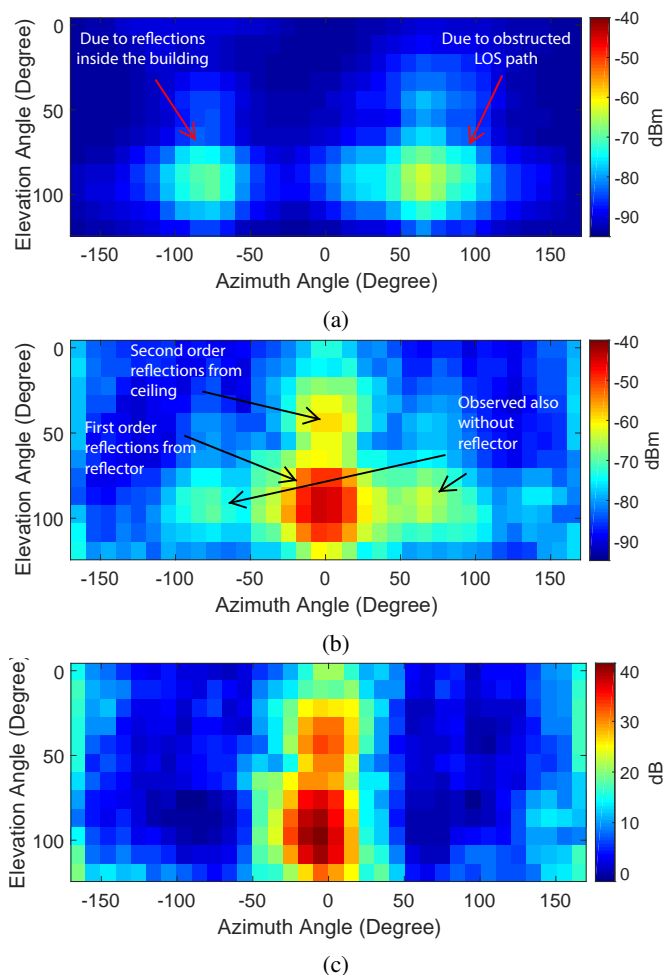


Fig. 8: Measurement results for (a) without reflector, (b) with reflector, (c) the gain obtained with reflector compared to no reflector case.

is measured by summing the power values from the PDP provided by the channel sounder. Fig. 8(a), shows the measured power when there is no reflector. In this case the maximum power which is -64 dBm is observed at the azimuth angle of 65° and an elevation angle of 87°. Furthermore, the signal is received with -70 dBm power at the same elevation angle and at -75° azimuth angle. The strongest path corresponds to the direct path between the transmitter and the receiver and the other path corresponds to some reflections inside the building.

Fig. 8(b) shows the measured power with the reflector in place. The two strong components when there is no reflector shows up in this case as well. However, here we observe the strongest received power of -45 dBm at azimuth angle of -5° and the same elevation angle of 87°. This is the first order reflection from the reflector. A second order reflection from the ceiling having a power of -59 dBm, is also observed at the elevation angle 44° and the same azimuth angle -5°. We observe that when the

reflector is used, the strongest power is increased by $(-45 \text{ dBm}) - (-64 \text{ dBm}) = 19 \text{ dB}$.

Finally, Fig. 8(c) plots the power gain obtained with reflector compared to without reflector by subtracting the results in Fig. 8(a) from the results in Fig. 8(b). We note that at the position where the receiver faces the reflector, around 40 dB gain is observed.

V. CONCLUSIONS

In this work, we have studied the effect of a passive metallic reflector to enhance the coverage for mmWave signals in an outdoor setting. The measurement results show that using 33 in×33 in metallic reflector, 19 dB gain in power is possible compared to no reflector case. Our future work includes extensive indoor/outdoor measurement campaigns to characterize the channel scattering properties for typical indoor/outdoor 5G communication environments.

REFERENCES

- [1] "Mobile fact sheet, pew research center," accessed: 7-30-2018. [Online]. Available: <http://www.pewinternet.org/fact-sheet/mobile/>
- [2] M. Kerker, *The scattering of light and other electromagnetic radiation*. Elsevier, 2016.
- [3] S. N. Ghosh, *Electromagnetic theory and wave propagation*. CRC Press, 2002.
- [4] Y. Huang, N. Yi, and X. Zhu, "Investigation of using passive repeaters for indoor radio coverage improvement," in *IEEE Ant. Propag. Society Sympos.*, vol. 2, June 2004, pp. 1623–1626 Vol.2.
- [5] J. L. D. L. T. Barreiro and F. L. E. Azpiroz, "Passive reflector for a mobile communication device," Aug. 2006, US Patent 7,084,819.
- [6] C. C. Cutler, "Passive repeaters for satellite communication systems," Feb. 9 1965, uS Patent 3,169,245.
- [7] J. L. Ryerson, "Passive satellite communication," *Proc. of the IRE*, vol. 48, no. 4, pp. 613–619, April 1960.
- [8] Y. E. Stahler, "Corner reflectors as elements passive communication satellites," *IEEE Trans. Aerospace*, vol. 1, no. 2, pp. 161–172, Aug. 1963.
- [9] J. Bjornholt, G. Hamman, and S. Miller, "Electronic fence using high-resolution millimeter-wave radar in conjunction with multiple passive reflectors," 15 2002, uS Patent 6,466,157.
- [10] W. Khawaja, K. Sasaoka, and I. Guvenc, "UWB radar for indoor detection and ranging of moving objects: An experimental study," in *Proc. IEEE Int. Workshop Ant. Technol. (iWAT)*, 2016, pp. 102–105.
- [11] C. Bredin, J.-M. Goutoule, R. Sanchez, J.-P. Aguttes, and T. Amiot, "High resolution SAR micro-satellite based on passive reflectors," in *Proc. IEEE Int. Geoscience and Remote Sensing Symposium*, vol. 2, 2004, pp. 1196–1199.
- [12] W. Khawaja, O. Ozdemir, Y. Yapici, I. Guvenc, and Y. Kakishima, "Coverage enhancement for mmWave communications using passive reflectors," in *Proc. IEEE Global Symp. Millimeter Waves (GSMM)*, Boulder, Colorado, May 2018.
- [13] S. Hiranandani, S. Mohadikar, W. Khawaja, O. Ozdemir, I. Guvenc, and D. Matolak, "Effect of passive reflectors on the coverage of IEEE 802.11ad mmWave systems," in *Proc. IEEE Vehic. Technol. Conf. (VTC) workshops*, Chicago, IL, Aug. 2018.
- [14] Z. Peng, L. Li, M. Wang, Z. Zhang, Q. Liu, Y. Liu, and R. Liu, "An effective coverage scheme with passive-reflectors for urban millimeter-wave communication," *IEEE Ant. Wireless Propag. Lett.*, vol. 15, pp. 398–401, 2016.
- [15] National Instruments, "mmWave Transceiver System," accessed: 7-31-2018. [Online]. Available: <http://www.ni.com/sdr/mmwave/>
- [16] Stanford Research Systems, "FS725 Rubidium Frequency Standard," accessed: 7-31-2018. [Online]. Available: <https://www.thinksrs.com/products/fs725.html>
- [17] SAGE Millimeter, Inc, "SAR-1725-34KF-E2 Rectangular Horn Antenna," accessed: 7-31-2018. [Online]. Available: <https://www.sagemillimeter.com/17-dbi-gain-wr-34-2-92-mm-female-connector-rectangular-horn-antenna/>
- [18] Flir Systems, "FLIR PTU-D48E Pan/Tilt Unit," accessed: 7-31-2018. [Online]. Available: <https://www.flir.com/products/ptu-d48e/>